Localization in random media and its effect on the homogenized behavior of materials

François Willot

Center for Mathematical Morphology
& Center for Materials P. M. Fourt

MINES ParisTech

SORBONNE UNIVERSITÉ

Soutenance d'Habilitation à Diriger des Recherches

Mines ParisTech, October 8 2019

Banding patterns in elasticity : cracked polycrystal

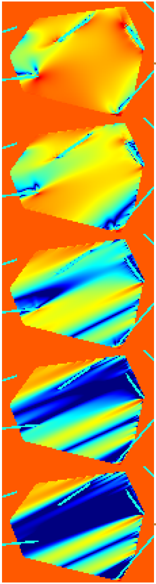

Onset of a low percolation threshold in polycrystals with hexagonal symmetry, as crystal anisotropy increases.

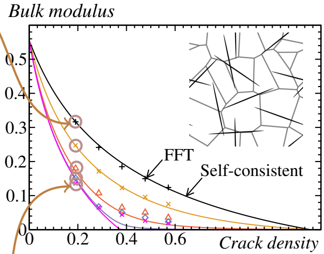

Interpreted as the development of weakly-loaded regions around cracks.

To which extent may homogenization theories be used to predict not only the self-consistent but the *entire* elastostatic probability distribution field ?

Refs : Barthelemy & Orland (1997), Cule & Torquato (1998), Idiart et al (2006), Giordano (2007)

Elastostatic probability field distributions

Homogeneous cracked body under plane strain & biaxial stress loading

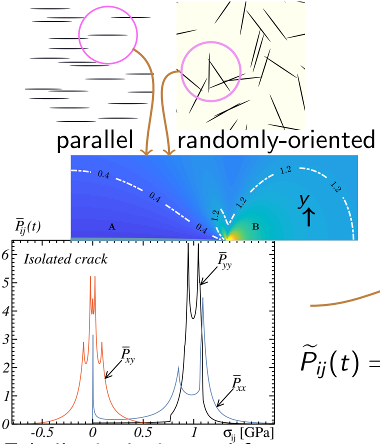

Eshelby inclusion p.d.f

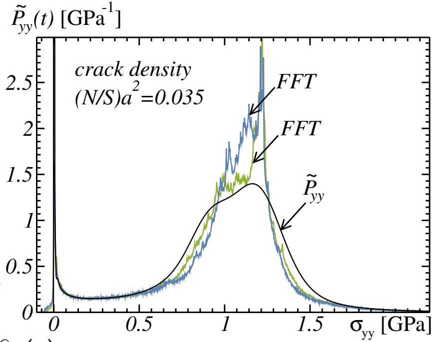

$$\widetilde{P}_{ij}(t) = \int_{-\infty}^{+\infty} \mathrm{d}s \frac{q(s)}{|s|} \underbrace{\overline{P}_{ij}\left(\frac{t}{s}\right)}_{\text{Eshelby inclusion}}$$

$$\langle t^n \rangle_q = \underbrace{\langle t^n \rangle_{\widetilde{P}_{ij}}}_{\text{FFT/self-consistent}} \Big/ \underbrace{\langle t^n \rangle_{\overline{P}_{ij}}}_{\text{Eshelby inclusion}}$$

Modeling of the stress intensity factor around each crack as a Gaussian probability distribution q. Van Hove singularities smoothed out, except at $\sigma_{ij} = 0^{\pm}$ and $\pm\infty$.

Elastostatic probability field distributions

Van Hove singularities for the Eshelby inclusion problem computed making use of asymptotic expansions of the local stress fields in regions of interest. Allows one to derive estimates for the corresponding singularities in the p.d.f. for populations of interacting cracks

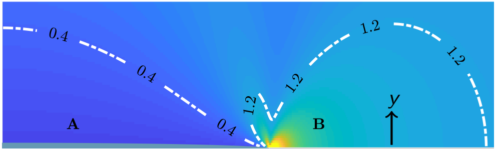

$$\widetilde{P}_{ij}(t) = \int_{-\infty}^{+\infty} \mathrm{d}s \, \frac{q(s)}{|s|} \overline{P}_{ij}\left(\frac{t}{s}\right)$$

<table>
<tr><th></th><th></th><th>Eshelby</th><th>parallel</th><th>randomly-oriented</th></tr>
<tr><td rowspan="3">$t = 0^{\pm} = \{$</td><td>σ_{xx}</td><td>$H(t)$</td><td>$-\log t$</td><td rowspan="2">$[a + bH(t)]|t|^{-1/3}$</td></tr>
<tr><td>σ_{yy}</td><td>$H(t)|t|^{-2/3}$</td><td>$[a + bH(t)]|t|^{-2/3}$</td></tr>
<tr><td>σ_{xy}</td><td>$|t|^{-1/2}$</td><td>$|t|^{-1/2}$</td><td>$\log^2 |t|$</td></tr>
<tr><td rowspan="2">$t = \pm\infty = \{$</td><td>$\sigma_{yy}, _{xx}$</td><td>$H(t)|t|^{-5}$</td><td colspan="2">$[a + bH(t)]|t|^{-5}$</td></tr>
<tr><td>σ_{xy}</td><td colspan="3">$|t|^{-5}$</td></tr>
</table>

$H(t)$: Heaviside function.

Powerlaw decay with exponent -5 for the distribution of the stress field.

Elastostatic probability field distributions

Comparison with Fourier numerical results. Crack density $\eta = Na^2/S = 0.035$

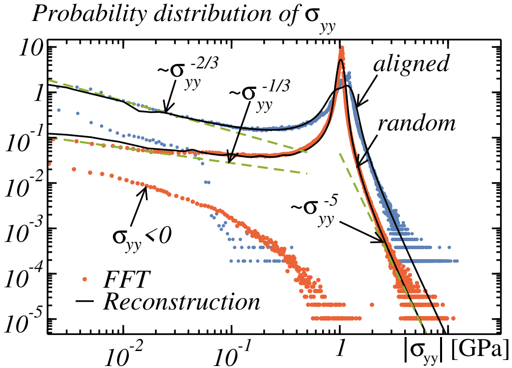

$t \to \pm\infty$:

$$\widetilde{P}_{yy}(t) \sim \frac{\omega\pi\eta}{|t|^5} \overbrace{\int_0^\infty \mathrm{d}s\, s^4 q(\mathrm{sign}(t)s)}^{\text{self. cons. \& Eshelby incl.}}$$

$$\omega = \begin{cases} 1089/512 & \text{(parallel)} \\ 585/512 & \text{(random)} \end{cases}$$

FFT data consistent with the scaling law $\sim t^{-5}$ when $t \to \pm\infty$ with much lower prefactor when $t \to -\infty$.

Analysis restricted to a low crack density. Local loadings in arbitrary directions, making use of a multivariate distribution q, not considered here.

Nonlinear random media : context and motivation

Emergence of *special flow paths* in model of nonlinear varistors (Roux et al, 1987 ; Donev et al, 2002). *Shortest path* and minimum cut problems, or minimal manifolds. Strain localization. Related problems in mechanics (e.g. damage induced by cracks).

A simple example : network of nonlinear conductors

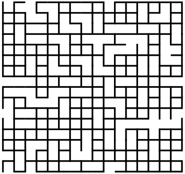

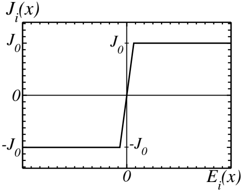

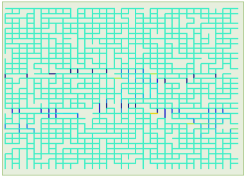

$$\chi_0 = \min_{\text{path } p} \sum_{i \in \mathrm{p}} J_0^{(i)}$$

Equivalence between effective current threshold and minimal path in the dual lattice

Problem : nonlinear conducting material *in the continuum* with randomly-distributed insulating (or highly-conducting) inclusions, in 2D. Anti-plane perfect plasticity.

Refs : Drucker (1966), Roux & François (1991), Roux & Hansen (1992), Ponte Castañeda & Suquet (1997), Donev et al (2002), Duxbury et al (2006), Jeulin & Ostoja-Starzewski (2007), Sillamoni & Idiart (2016), Furer & Ponte Castañeda (2018)

Boolean model of disks : shortest path

Equisized disks of radius D, homogeneous Poisson point process of intensity θ. Join points $\boldsymbol{A}$ to $\boldsymbol{B}$ by a path passing through disk with centers $\boldsymbol{C}^i$

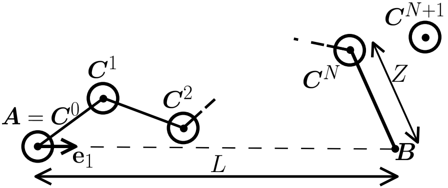

Corresponding upper-bound :

$$\xi \leq \frac{\sum_{i=1}^{N}\left(\sqrt{\ell_i^2 + m_i^2} - D\right) + Z}{\sum_{i=1}^{N} \ell_i}$$

Idea : choose disk $\boldsymbol{C}^{i+1}$ in the region :

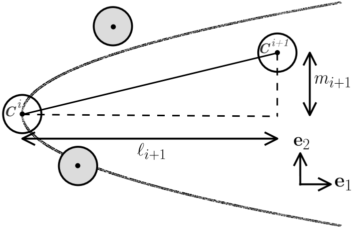

$$|C_1^{i+1} - C_1^i| = \inf\Big\{|C_1 - C_1^i|;\ \ \boldsymbol{C} \text{ a disk center}\,;$$

$$C_1 > C_1^i + D,\ |C_2 - C_2^i| \leq b\sqrt{D|C_1 - C_1^i|}\Big\}.$$

b to be optimized on

Geodesics in the Boolean model of disks

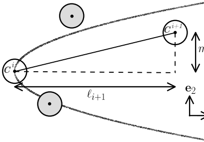

Upper bound obtained by :

$$P\{\ell_i > \ell\} = \exp(-\theta\mu_2(K))$$

with K =domain enclosed by the two $\sqrt{}$ curves and the line $\ell = \ell_i$.
Sharpest bound obtained with the choice $b = \sqrt{3/2}$:

$$\xi \le 1 - \frac{3}{\Gamma\left(\frac{2}{3}\right)}\left(\frac{3f}{2\pi}\right)^{2/3} + O(f^{4/3}) \approx 1 - 1.3534 f^{2/3}, \qquad f \to 0$$

Boolean model of arbitrary grain and "cost" $0 < p < 1$ in the grains :

$$\xi \quad \le \quad 1 - (1-p)^{4/3}\frac{3^{5/3}}{4\Gamma\left(\frac{2}{3}\right)}\left(\frac{w_g^2 f}{A_g}\right)^{2/3}$$

$$\xi \quad \le \quad 1 - (1-p)f$$

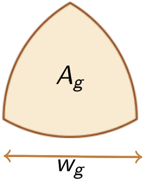

Consistent with numerical computations & "second-order" nonlinear homogenization theory in the anti-plane problem (up to numerical pre-factor)

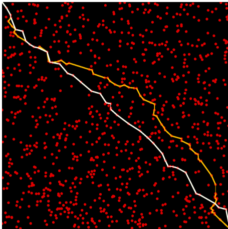

Two-scale Cox-Boolean model

Boolean model of disks aggregated into clusters

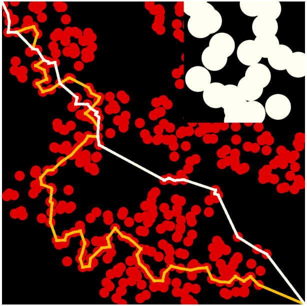

$$f = f_{\text{clus}} f_{\text{in}}, \quad f_{\text{clus}}, f_{\text{in}} \ll 1$$

Dilute limit expansion :

$$\xi \leq 1 - \alpha(1-p)^{4/3} f_{\text{clus}}^{2/3}, \qquad \alpha = 1.35$$

Numerical computations :

$$\xi \approx 1 - \alpha(1-p)^{4/3} f_{\text{clus}}^{2/3}, \qquad \alpha = 1.85$$

Scale separation : $p \approx 1 - \alpha f_{\text{in}}^{2/3}$

Dilute expansion for the two-scale model :

$$\boxed{\xi \approx 1 - \max\left\{\alpha^{7/3} f_{\text{in}}^{8/9} f_{\text{clus}}^{2/3}, \alpha f_{\text{in}}^{2/3} f_{\text{clus}}\right\}}$$

Two-scale Cox-Boolean model

Bounds prediction
in the dilute limit

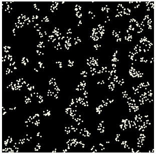

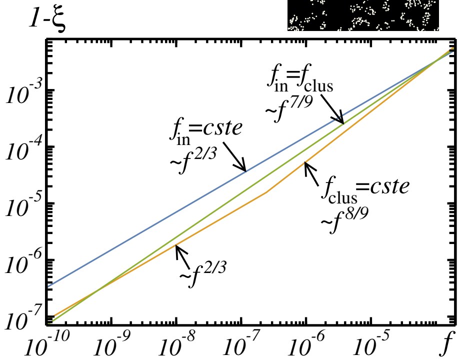

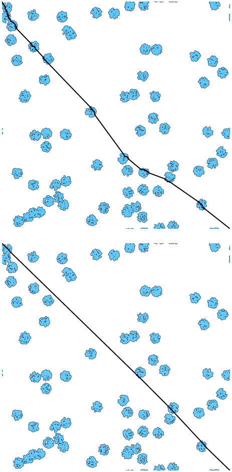

Regime change when $f_{\text{clus}} = cste$ and f_{in} varies. Related to the presence and absence of rugosity at the macroscopic scale.

Two-scale Cox-Boolean model

Comparison with numerical results in the case $f_{\text{clus}} = cste$. Varying values of f_{clus}.

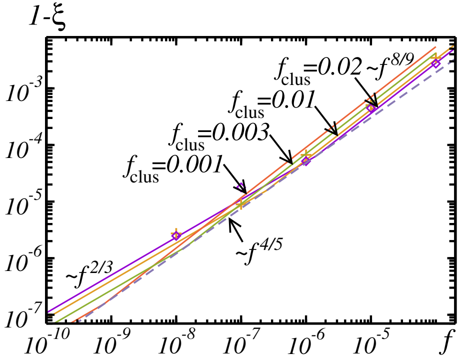

Lowest effect of the voids in two-scale media observed at the regime change ($f_{\text{in}}^{2/3} \sim f_{\text{clus}}$) in which case $1 - \xi \sim f^{4/5}$.

N-scale Cox-Boolean model

Pores embedded in clusters of pores embedded in super clusters, etc.
Total porosity : $f = f_1 \dots f_N$. Let $f_i = f^{\beta_i}$ ($\sum_i \beta_i = 1$).

$$1-\xi \sim f^{\nu_1}, \quad \nu_N = \frac{2\beta_N}{3}, \quad \nu_i = \nu_{i+1} + \frac{2}{3}\beta_i + \frac{1}{3}\min\left\{\beta_i ; \nu_{i+1}\right\}, \quad 1 \le i < N.$$

Properties : $2/3 \le \nu_1 \le (1+2^{-N})^{-1} \to 1$ ($N \to \infty$).

- Lowest exponent (i.e. highest effect of the pores) obtained when $\beta_1 = 1$ (clusters fraction decrease very slowly except at the highest scale) or $\beta_N = 1$ (clusters fraction decrease very slowly except at the lowest scale).
- Highest exponent (i.e. lowest effect of the pore) obtained when $\beta_i = \nu_{i+1}$. However, as $N \to \infty$ "almost" any choice of β_1 leads to $\nu_1 \approx 1$, i.e. **a linear correction**.

Model of rigid grains

Rigid grains (minimal paths avoid grains)

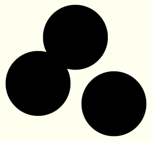

Boolean model

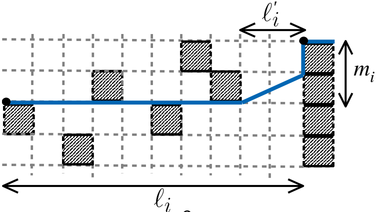

$\xi \leq 1 - (\log f) f^3, \qquad f \to 0.$

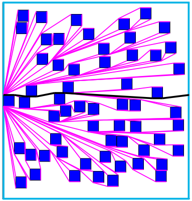

Random sequential adsorption model of squares.

$\xi \approx 1 + f^2/32, \quad f \to 0$
(non-rigorous analysis)

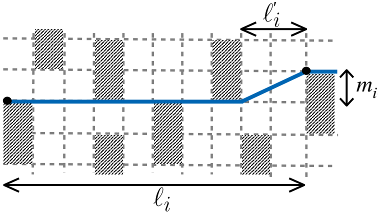

$\xi \leq 1 - \frac{3}{8}(\log f) f^2, \qquad f \to 0.$

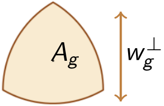

$\xi \approx 1 + \frac{(w_g^\perp)^4}{32 A_g^2} f^2, \quad f \to 0$
(grains with moderate aspect ratio)

RSA model of squares

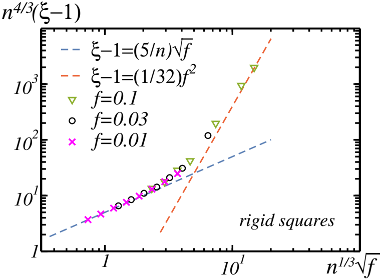

Numerical data collapse (n the number of squares in the numerical simulation)
Consistent with the scaling law

$$\xi \approx 1 + (1/32)f^2, \qquad f \to 0$$

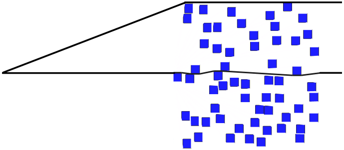

For squares with cost $p > 1$

$$\xi \approx 1 + \min\left\{(1/32)f^2, (p-1)f\right\}$$

For a N-scale model of rigid squares ($f = f_1 \dots f_N$, $f_i = f_i^{\beta}$, $\sum_i \beta_i = 1$)

$$\xi - 1 \sim f^{\nu}, \quad \nu = \beta_1 + \max(\beta_1, \beta_2 + \max(\beta_2, \beta_3 + \dots + \max(\beta_{N-1}, 2\beta_N)\dots)$$

with $1 \le \nu \le 2$. Minimal value of ν (maximal effect of the inclusions) obtained when $\beta_i = 2\beta_{i+1}$. As $N \to \infty$, $\nu \to 1$ for almost all choices of β_i. Consistent with the bound $Y_0/Y \le 1 + (7/2)f$ (Goldsztein, 2011)

Stokes flow in porous media

Boolean model of oblate cylinders with high aspect ratio, and high volume fraction

Pores/
cylinders

Obstacles
(vol. frac.
q)

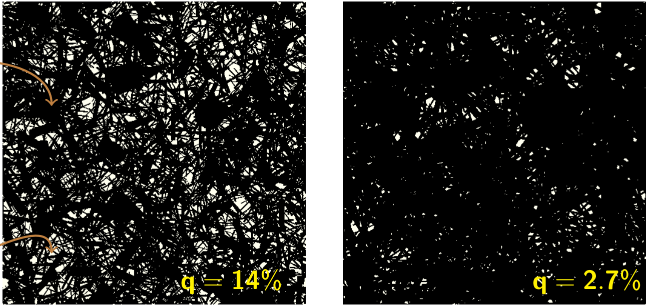

Stokes flow (viscosity μ, pressure p, velocity field $\vec{u}$)

$$\mu \Delta \vec{u} = \vec{\nabla} p, \quad \langle \vec{u} \rangle = -\frac{k}{\mu} \langle \vec{\nabla} p \rangle$$

Stokes flow in porous media

Berryman-Milton bound : $k \leq \frac{2}{3q^2} \int_0^\infty \mathrm{d}t\, t \left[F_{vv}(t) - q^2\right]$

Covariance function : $F_{vv}(t = |\boldsymbol{t}|) = P\{\boldsymbol{x}, \boldsymbol{x} + \boldsymbol{t} \in \text{Obstacles}\} = q^{2-K(t)}$

Geometrical covariogram of the cylinder C (radius r, height h) :

$$K(t) = E\left\{\frac{|C \cap C_r|}{|C|}\right\} \approx \begin{cases} 1 - \frac{(r+h)t}{2rh} + \frac{2t^2}{3\pi rh} & \text{if} \quad t < h, \\ \left(\frac{h^2}{6t^2} - 1\right) \frac{h}{2\pi r} \sqrt{1 - \frac{t^2}{4r^2}} + \frac{h}{\pi t} \cos^{-1}\frac{t}{2r} & \text{if} \quad t > h. \end{cases}$$

In the limit of infinitesimal volume fraction of obstacles and very large aspect ratios, two regimes appear :

$$k \leq \begin{cases} \frac{8h^2}{3q(\log q)^2}\left[1 + \left(\frac{1}{2}\log q - 1\right)\sqrt{q}\right] & q \to 0 \text{ and afterwards } r \to \infty, \\ -\frac{8hr}{9\pi}\log q & r \to \infty \text{ and afterwards } q \to 0 \end{cases}$$

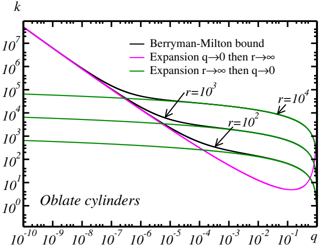

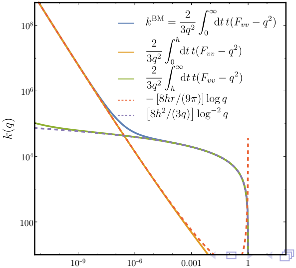

Slow increase of k with q in the regime $r \gg r_c$

$r_c = -h/(q \log^3 q)$

Stokes flow in porous media

Berryman-Milton bound dilute expansion :

$$k \leq \begin{cases} \frac{8h^2}{3q(\log q)^2}\left[1+\left(\frac{1}{2}\log q - 1\right)\sqrt{q}\right] & r \ll r_c, \\ -\frac{8hr}{9\pi}\log q & r \gg r_c \end{cases}$$

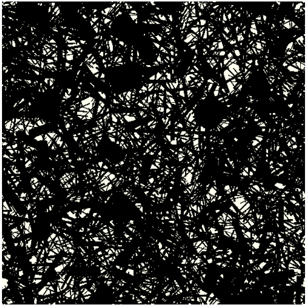

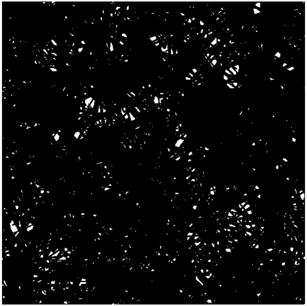

Fluid flow constrained to lie inside "chanels" (cylinders) when $r \gg r_c$ ($k \sim hr$, k monitored by the tail of F_{vv}). Fluid flow becomes unconstrained (flow around isolated obstacles) when $r \ll r_c$ ($k \sim h^2$, k monitored by $F_{vv}(t)$ in the domain $0 < t < h$)

Conclusion

- A link has been established between the effective yield stress (in anti-plane shear) in porous and rigidly-reinforced perfectly-plastic media and homogenized metrics
- Possible scenario for the localization bands in random particulate media with dilute concentration of inclusions
- A “greedy” path gives scaling laws consistent with nonlinear homogenization theories and with numerical results. In particulate random microstructures, the method predicts corrections from $\sim f^{2/3}$ (homogeneously-distributed pores) to $\sim f$ (aggregated pores at many different scales).
- In multiscale structures, the value of the exponent depends on whether the minimal path exhibits a rugosity at the various scales. Regime changes are observed when rugosity appears at a given scale.
- The lowest effect of pores (highest exponent) is obtained when the particle distribution corresponds to a regime change simultaneously at all scales.
- Regime change for Stokes flow in porous media with long-range correlations induced by the spatial distribution of obstacles
- Reconstruction of the local elastic fields in heterogeneous media. Banding patterns in linear media with non-strictly convex potentials.